Robust Control Barrier Functions for Safety Using a Hybrid Neuroprosthesis

Krysten Lambeth, Mayank Singh, and Nitin Sharma*

Abstract—Many lower-limb hybrid neuroprostheses lack powered ankle assistance and thus cannot compensate for functional electrical stimulation-induced muscle fatigue at the ankle joint. The lack of a powered ankle joint poses a safety issue for users with foot drop who cannot volitionally clear the ground during walking. We propose zeroing control barrier functions (ZCBFs) that guarantee safe foot clearance and fatigue mitigation, provided that the trajectory begins within the prescribed safety region. We employ a backstepping-based model predictive controller (MPC) to account for activation dynamics, and we formulate a constraint to ensure the ZCBF is robust to modeling uncertainty and disturbance. Simulations show the superior performance of the proposed robust MPC-ZCBF scheme for achieving foot clearance compared to traditional ZCBFs and Euclidean safety constraints.

I. Introduction

Powered exoskeletons and functional electrical stimulation (FES) are often prescribed as rehabilitative interventions for neuromuscular conditions such as spinal cord injury [1], [2] and stroke [3]. FES has been shown to reduce spasticity [1] and improve mobility [2]; however, the artificial recruitment of the muscles leads to rapid muscle fatigue [4]. This fatigue can be reduced by using FES in conjunction with an exoskeleton [5], [6]. Furthermore, the use of FES reduces the torque and power required from the exoskeleton motors [5], [7]. Such a device, termed a hybrid neuroprosthesis, is challenging to control because the joints are often overactuated; they can be controlled by both FES and exoskeleton motors. One means to address the overactuation problem is model predictive control (MPC), which has been successfully employed for hybrid neuroprostheses [8]-[10]. MPC uses a model of the system to calculate the optimal control inputs for some prediction horizon comprised of N > 1 time steps, but only the solution for the first timestep is applied at each iteration. Future prediction and cost minimization are considered when making the immediate control decision. MPC also allows for straightforward incorporation of state and control constraints.

Safety is another critical constraint highly relevant to systems using FES and powered exoskeletons for rehabilitation. Various safety concerns, including delivering limited assistance, ground reaction force, and human-robot interaction

K. Lambeth and N. Sharma are with the UNC/NC State Joint Department of Biomedical Engineering, NC State University, Raleigh, NC 27606 USA (e-mail: kflambet@ncsu.edu). M. Singh is with the NC State Department of Electrical and Computer Engineering, NC State University, Raleigh, NC 27606 USA (e-mail: msingh25@ncsu.edu).

*Corresponding author: Nitin Sharma. This work was funded by NSF Award #2124017 and by NSF CAREER Award #2002261.

979-8-3503-2806-6/\$31.00 ©2023 AACC

force, have arisen in FES and exoskeleton safety and feasibility studies [11], [12]. To accurately determine human-robot interaction forces, [13] created contact models using data from sit-to-stand tasks with a multi-joint lower-limb exoskeleton, and [12] developed soft sensors that measured the human-hip exoskeleton interaction force online. An RGB-D camera was used in [14] to identify ground features and inform exoskeleton motion planning subject to allowed step lengths and obstacle avoidance, while [15] analyzed lower-limb exoskeleton fall strategies under various conditions. [16] developed a saturated controller for an FES cycle that prevented overstimulation and possible destabilization due to the delay between stimulation onset and muscle contraction. Also, for FES cycling, [17] applied motor assistance once FES reached the saturation level to avoid overstimulation. A control barrier function (CBF) was employed in [18] to keep the FES cycling cadence within a safe range. CBFs have been combined with control Lyapunov functions in quadratic programs to achieve performance objectives while maintaining safety during bipedal robotic walking [19]. CBFs have also been used in MPC [20], which often offers more optimal solutions compared to quadratic programs due to its consideration of future state behavior [21].

In an MPC scheme, a simple obstacle avoidance constraint may be formulated as $(x-x_0)^2+(y-y_0)^2-D^2\geq 0$, where $(x_0,y_0)\in\mathbb{R}^2$ is the obstacle location, $(x,y)\in\mathbb{R}^2$ is the location of the user's foot, and $D\in\mathbb{R}^+$ is the minimum safe distance. A limitation of such a safety constraint is that it only affects the optimal control solution once the constraint becomes active within the prediction horizon. In other words, the safety constraint does not affect the solution until the robot is already closing in on the obstacle [22]. Furthermore, MPC cannot ensure that the constraints are respected beyond the prediction horizon. An obvious solution to these problems is to lengthen the time horizon, but this poses a substantial increase in computational cost for high-dimensional, highly nonlinear systems such as hybrid neuroprostheses [23].

CBFs, in contrast, ensure that if the safety parameters are satisfied at some initial time t_0 , they remain satisfied for all time [24]. Specifically, CBFs guarantee forward invariance of the safe set by bounding the derivative of the safety constraint. The two common formulations of CBFs are zeroing CBFs (ZCBFs) and reciprocal CBFs. Of the two, ZCBFs are preferable for real-time control. This is because a ZCBF's value vanishes at the boundary of the safe set, whereas a reciprocal CBF's value grows infinitely at the boundary. A modified formulation of ZCBFs was proposed in [19] that permits a greater number of admissible inputs while still

guaranteeing safety, thus increasing the likelihood that the ZCBF-MPC will be recursively feasible. Further modification to the discrete-time formulation of ZCBF-MPC was presented in [20], where the decay rate of the CBF was treated as a decision variable. This further increases the probability that the intersection of the safe and reachable sets is nonempty and thus that the problem is feasible.

In this paper, we employ ZCBFs to address the issue of foot drop in a walking task for a hybrid neuroprosthesis. Foot drop refers to impaired dorsiflexion, common to many neuromuscular disorders. Most state-of-the-art lower-limb hybrid neuroprostheses do not possess motors at the ankle joint, as this would add to the system's inertia. Instead, a rigid anklefoot orthosis is typically used to prevent the foot from scuffing the ground due to insufficient dorsiflexion during walking. However, this results in an unnatural gait since the ankle joint is immobilized. In contrast, we wish to permit the ankle joint to move with assistance from FES, which is commonly used to treat foot drop and can also help reduce ankle muscle spasticity [25], [26]. Without an ankle motor to provide synergistic torque across limbs as needed, it is imperative that the controller consider ankle muscle fatigue. Unlike the ankle, the hip and knee joints possess motors and can compensate for fatigue. If the dorsiflexors are too fatigued to achieve foot clearance, the MPC with embedded CBF should respond by increasing hip and knee flexion. Furthermore, the inclusion of an obstacle clearance constraint obviates the need to replan the desired time-varying trajectory. The optimal path is the one that reaches the desired endpoint the fastest without violating the safety constraints.

Our multi-joint MPC scheme for a hybrid neuroprosthesis walking task incorporates a foot clearance ZCBF and fatigue ZCBFs that constrain the FES-induced fatigue of the ankle dorsiflexors and plantar flexors. We first develop a nonlinear MPC for a control non-affine hybrid neuroprosthesis through a backstepping-based method, followed by the derivation of three ZCBFs. Utilizing the method for creating input-to-state safe CBFs [27], we then formulate a condition to ensure that the true system remains in the safe set despite disturbance and modeling uncertainty.

II. PROBLEM FORMULATION

A. 3-Link Hybrid Neuroprosthesis Model

Consider a hybrid neuroprosthesis with thigh, shank, and foot segments. The vector $q \in \mathbb{R}^3$ contains the limb segment angles q_i (i = 1, 2, 3). The neuroprosthesis possesses hip and knee motors (represented by subscripts i = hm, km, respectively), and FES is used to actuate the knee flexors, knee extensors, ankle plantar flexors, and ankle dorsiflexors (j = kf, ke, pf, and df, respectively). The model dynamics are given as

$$M(q)\ddot{q} + C(q,\dot{q})\dot{q} + F(q,\dot{q}) + G(q) + d(t) = \Gamma(t),$$
 (1)

an unmodeled disturbance. The active torque from FES and motors, $\Gamma(t) \in \mathbb{R}^3$, is calculated as

$$\Gamma = b(q, \dot{q})\mu a(t),$$

where $b(q,\dot{q}) \in \mathbb{R}^{3 \times 6}$ is a mapping matrix, $\mu \in \mathbb{R}^{6 \times 6}$ is a diagonal fatigue matrix, and $a(t) \in \mathbb{R}^6$ is the vector of FES and motor activations. Mapping matrix b is given as

$$b(q,\dot{q}) = \begin{bmatrix} \kappa_h & 0 & 0 & 0 & 0 & 0 \\ 0 & \psi_{kf} & -\psi_{ke} & \kappa_k & 0 & 0 \\ 0 & 0 & 0 & \psi_{pf} & -\psi_{df} \end{bmatrix},$$

where $\kappa_h, \kappa_k \in \mathbb{R}^+$ are the hip and knee motor constants, respectively, and $\psi_j(q_j,\dot{q}_j) \in \mathbb{R}$ are the muscle torquelength/torque-velocity equations from [28], [29]. The hip is not actuated by FES due to the fact that the hip flexors/extensors are difficult to actuate non-invasively. As mentioned in Section I, there is no motor at the ankle joint. Fatigue matrix μ is represented as

$$\mu = diag([1, \mu_{kf}, \mu_{ke}, 1, \mu_{pf}, \mu_{df}]),$$

where $\mu_j \in [\mu_{min_j}, 1]$ and $\mu_{min_j} \in (0, 1)$ are the fatigue state and minimum fatigue value, respectively, for actuator j. The fatigue dynamics is

$$\dot{\mu} = T_f^{-1}(\mu_{min} - \mu)a + T_r^{-1}(I - \mu)(1 - a), \tag{2}$$

where $T_f, T_r \in \mathbb{R}^{6 \times 6}$ are diagonal matrices of fatigue and recovery time constants $T_{f_i}, T_{r_i} \in \mathbb{R}^+$, respectively, and $\mu_{min} = diag([1, \mu_{min_{kf}}, \mu_{min_{ke}}, 1, \mu_{min_{pf}}, \mu_{min_{df}}]) \in$ $\mathbb{R}^{6\times 6}$. The activation dynamics is

$$\dot{a} = T_{act}^{-1}(u - a),\tag{3}$$

where $T_{act} \in \mathbb{R}^{6 \times 6}$ is the diagonal matrix of activation time constants $T_{act_j} \in \mathbb{R}^+$ and $u(t) \in \mathbb{R}^6$ is the normalized current input. For FES, $a_j, u_j \in [0, 1]$, whereas for motors $a_j, u_j \in$

Assumption 1: Desired joint trajectories $q_d(t) \in \mathbb{R}^3$, as well as their first and second time derivatives, are bounded.

Assumption 2: Desired activation trajectories $a_d(t) \in \mathbb{R}^6$ and their first derivatives are bounded.

B. Task-Space Dynamics

Because it is critical to achieve foot clearance during the swing phase, we formulate the swing dynamics in a task-space, also known as endpoint space. This can be done by invoking the Jacobian of the endpoint, $J(q) \in \mathbb{R}^{2\times 3}$, which maps \dot{q} to $\dot{z} \in \mathbb{R}^2$ as $\dot{z} = J(q)\dot{q}$, where \dot{z} is the Cartesian velocity of the endpoint in the sagittal and frontal planes. Letting $z \in \mathbb{R}^2$ be the endpoint position, (1) when written in task-space is

$$M_z(z)\ddot{z} + C_z(z,\dot{z})\dot{z} + F_z(z,\dot{z}) + G_z(z) + d_z(t)$$
 (4)
= $b_z(z,\dot{z})\mu a(t)$,

where $M(q) \in \mathbb{R}^{3 \times 3}$ is the inertia matrix, $C(q,\dot{q}) \in \mathbb{R}^{3 \times 3}$ is $M(q) \in \mathbb{R}^{3 \times 3}$ is where $M_z = (J^T)^\dagger M J^\dagger$, $C_z = (J^T)^\dagger (C - M J^\dagger \dot{J}) J^\dagger \in \mathbb{R}^{3 \times 3}$ the Coriolis matrix, $F(q,\dot{q}) \in \mathbb{R}^3$ is the passive muscle torque $\mathbb{R}^{2 \times 2}$, $F_z = (J^T)^\dagger F$, $G_z = (J^T)^\dagger G$, $G_z = (J^T)^\dagger G$, and as in [28], $G(q) \in \mathbb{R}^3$ is the gravitational torque, and $G(z) = (J^T)^\dagger G$.

C. Nominal Error Dynamics

Preliminary 1. Let \bar{v} represent the nominal counterpart of a given value v. (Note that "nominal" here refers to the case when d(t) in (1) is zero.)

Preliminary 2. A continuous function $\rho:[0,a)\to[0,\infty)$ is class \mathcal{K} $(\rho\in\mathcal{K}_{[0,a)})$ if it is strictly increasing and $\rho(0)=0$.

The control objective is to minimize trajectory error while (a) preventing rapid ankle fatigue and (b) ensuring foot clearance. To this end, we define nominal trajectory error $e \in \mathbb{R}^2$ as

$$e = z_d - \bar{z},\tag{5}$$

where $z_d \in \mathbb{R}^2$ is the desired endpoint position. Furthermore, an auxiliary error $r \in \mathbb{R}^2$ is given by

$$r = \dot{e} + \alpha e,\tag{6}$$

where $\alpha \in \mathbb{R}^+$ is a user-defined gain. The nominal error dynamics may be written as

$$\bar{M}_z \dot{r} = \bar{M}_z (\ddot{z}_d + \alpha \dot{e}) + \bar{C}_z \dot{\bar{z}} + \bar{F}_z + \bar{G}_z - \bar{b}_z \bar{\mu} \bar{a}. \tag{7}$$

Next, auxiliary functions $N, N_d \in \mathbb{R}^2$ are defined as

$$N_d = M_z(z_d)\ddot{z}_d + C_z(z_d, \dot{z}_d)\dot{z}_d + F_z(z_d, \dot{z}_d) + G_z(z_d)$$

$$N = \bar{M}_z(\ddot{z}_d + \alpha \dot{e}) + \bar{C}_z(\dot{z}_d + \alpha e) + \bar{F}_z + \bar{G}_z + e.$$

Note that N_d may also be written as $N_d = b_z(z_d, \dot{z}_d)\mu_d a_d$, where diagonal matrix $\mu_d \in \mathbb{R}^{6 \times 6}$ contains the desired constant muscle fatigue values $\mu_{d_j} \in [\mu_{min_j}, 1]$. Defining $\tilde{N} \in \mathbb{R}^2$ as $\tilde{N} = N - N_d$, the terms N_d and $\bar{b}_z \mu_d a_d$ may be added and subtracted so that (7) becomes

$$\bar{M}_z \dot{r} = \tilde{N} - \bar{C}_z r - \tilde{b} \mu_d a_d - \bar{b}_z \bar{\mu} \bar{a} + \bar{b}_z \mu_d a_d - e, \quad (8)$$

where $\tilde{b} \in \mathbb{R}^{2 \times 6}$ is defined as $\tilde{b} = \bar{b}_z - b_z(z_d, \dot{z}_d)$.

1) Backstepping Error Dynamics: Because the system is non-affine in the actuator input u, a backstepping error $e_x \in \mathbb{R}^6$ is introduced. The backstepping error is given as $e_x = \bar{a} - a_v$ for virtual input $a_v(t) \in \mathbb{R}^6$. By adding and subtracting $\bar{b}_z \bar{\mu} a_v$, (8) simplifies as

$$\bar{M}_z \dot{r} = \tilde{N} - \bar{C}_z r - \tilde{b}\mu_d a_d - \bar{b}_z \bar{\mu} e_x + \bar{b}_z \mu_d a_d - \bar{b}_z \bar{\mu} a_v - e. \tag{9}$$

To stabilize the system, the virtual input is defined as $a_v = \bar{\mu}^{-1} \mu_d a_d + k_1 (\bar{b}_z \bar{\mu})^{\dagger} r$, where $k_1 \in \mathbb{R}^+$ is a user-defined gain. (9) thus becomes

$$\bar{M}_z \dot{r} = \tilde{N} - \bar{C}_z r - \tilde{b} \mu_d a_d - \bar{b}_z \bar{\mu} e_x - e - k_1 r. \tag{10}$$

According to (3), the backstepping error dynamics is

$$\dot{e}_x = T_{act}^{-1}(u - \bar{a}) - \dot{a}_v. \tag{11}$$

The input u is designed as

$$u = \bar{a} + T_{act}(\dot{a}_v + \nu), \tag{12}$$

where $\nu(t) \in \mathbb{R}^6$ is the variable optimized by the MPC. Substituting (12) into (11), the backstepping error dynamics simplifies to

$$\dot{e}_r = \nu. \tag{13}$$

Finally, we introduce a fatigue error $\tilde{\mu} = [\bar{\mu}_{pf} - \mu_{d_{pf}}, \bar{\mu}_{df} - \mu_{d_{df}}]^T \in \mathbb{R}^2$, where $\mu_{d_i} \in [\mu_{min_j}, 1]$ is the desired value of

 μ_j . The nominal error dynamics may be written in state space as $\dot{\bar{x}} = f(\bar{x}) + g(\bar{x})\nu$, where $\bar{x} = [e^T, r^T, e_x^T, \tilde{\mu}^T]^T \in \mathbb{X}$, with $\mathbb{X} \subset \mathbb{R}^{12}$ the compact set of allowable states. Recalling (2), (6), (10), and (13), $f(x) \in \mathbb{R}^{12}$ and $g(x) \in \mathbb{R}^{12 \times 6}$ are defined as

$$f(x) = \begin{bmatrix} r - \alpha e \\ \bar{M}_z^{-1} (\tilde{N} - \bar{C}_z r - \tilde{b} \mu_d a_d - \bar{b}_z \bar{\mu} e_x - e - k_1 r) \\ 0 \\ T_{f_a}^{-1} (\mu_{min_a} - \Delta \mu_a) (e_{x_a} + a_{v_a}) + \\ T_{r_a}^{-1} (I - \Delta \mu_a) (1 - e_{x_a} - a_{v_a}) \end{bmatrix},$$
(14)

$$g(x) = \begin{bmatrix} 0_{4 \times 6} \\ I_6 \\ 0_{2 \times 6} \end{bmatrix},$$

where $\Delta \mu_a = diag([\bar{\mu}_{pf}, \bar{\mu}_{df}]) \in \mathbb{R}^{2 \times 2}$, and $T_{f_a}, T_{r_a}, \mu_{min_a} \in \mathbb{R}^{2 \times 2}$, $e_{x_a}, a_{v_a} \in \mathbb{R}^2$ are the elements of T_f, T_r, μ_{min}, e_x , and a_v corresponding to $\tilde{\mu}$.

III. CONTROL BARRIER FUNCTION

A. Zeroing Control Barrier Functions

The closed set $\mathcal{C} \subset \mathbb{X}$ pertaining to the continuously differentiable function $h(x) : \mathbb{X} \to \mathbb{R}$, is given by

$$C = \{\bar{x} \in \mathbb{X} : h(\bar{x}) \ge 0\},$$

$$\partial C = \{\bar{x} \in \mathbb{X} : h(\bar{x}) = 0\},$$

$$Int(C) = \{\bar{x} \in \mathbb{X} : h(\bar{x}) > 0\},$$
(15)

where $\mathbb{X} \subseteq \mathbb{R}^n$ is the compact set of all allowable states. We assume that \mathcal{C} is nonempty and contains no isolated points. \mathcal{C} is forward invariant and "safe" if $\bar{x}(t_0) \in \mathcal{C}$ at some time t_0 guarantees that $\bar{x}(t) \in \mathcal{C}$, $\forall t \geq t_0$. The function $h(\bar{x})$ is a zeroing control barrier function (ZCBF) defined on $\mathcal{D} \supset \mathcal{C}$ where $\mathcal{D} \subseteq \mathbb{X}$ if there exists $\gamma \in \mathcal{K}_{[0,a)}$ such that

$$\sup_{\nu \in \mathbb{U}} \left[L_f h(x) + L_g h(x) \nu \right] \ge -\gamma \left(h(\bar{x}) \right), \tag{16}$$

 $\forall \bar{x} \in \mathcal{D}$. We introduce the constant b > 0, given by

$$b = -\inf_{\bar{x} \in \mathbb{X}} h(\bar{x}),\tag{17}$$

and define the domain of h as the open set

$$\mathcal{D} = \{\bar{x} \in \mathbb{X} : h(\bar{x}) + b > 0\}. \tag{18}$$

In the absence of modeling error or disturbance (i.e., $\bar{x}=x$), (16) guarantees forward invariance of $\mathcal C$ because in the extreme case where $x\in\partial\mathcal C$, the constraint becomes $\dot{h}(x)\geq 0$. Thus, the state can never leave $\mathcal C$. If modeling error is present, it is necessary to modify (16) to account for discrepancy between the true and nominal states. For this purpose, we assume that the error term $\omega(t)$ is bounded by constant $\bar{\omega}\in\mathbb R^+$ as $||\omega_\infty||\leq \bar{\omega}$. Define a new set $\mathcal C'\supseteq \mathcal C$ as

$$C' = \{\bar{x} \in \mathbb{X} : h(\bar{x}) + \varphi(||\omega_{\infty}||) \ge 0\}$$

$$\partial C' = \{\bar{x} \in \mathbb{X} : h(\bar{x}) + \varphi(||\omega_{\infty}||) = 0\}$$

$$Int(C') = \{\bar{x} \in \mathbb{X} : h(\bar{x}) + \varphi(||\omega_{\infty}||) > 0\}$$

for $\varphi \in \mathcal{K}_{[0,a)}$, where a>0 satisfies $\lim_{v\to a} \varphi(v)=b$. Note that the choice of a guarantees that $\mathcal{C}'\subset \mathcal{D}$. As long as $x\in \mathcal{C}'$, x remains in \mathcal{C} or within a small neighborhood around \mathcal{C} .

B. Robust Obstacle Clearance Barrier Function

The purpose of the first barrier function is to achieve foot clearance. Here, we extend the problem to avoiding collision with an obstacle of arbitrary shape. The obstacle is centered at $z_c = [z_{c_1}, z_{c_2}] \in \mathbb{R}^2$, and a safety radius $R \in \mathbb{R}^+$ is established around the object. The safety constraint $h_1 : \mathbb{X} \to \mathbb{R}$ for the nominal MPC is therefore

$$h_1(\bar{x}) = (\bar{z}_1 - z_{c_1})^2 + (\bar{z}_2 - z_{c_2})^2 - R^2 \ge 0,$$
 (20)

where $\mathbb{X} \subset \mathbb{R}^{12}$. (20) may be written in terms of the error states as

$$h_1(\bar{x}) = ||z_d - e - z_c||^2 - R^2 \ge 0.$$
 (21)

Note that even if the nominal constraint is met, depending on \bar{z} and the magnitude of the modeling error, the true system may still lie outside \mathcal{C}_1 . Define the error in position $\epsilon(t) \in \mathbb{R}^2$ as

$$\epsilon = \bar{z} - z,\tag{22}$$

and define an auxiliary error $\delta(t) \in \mathbb{R}^2$ as

$$\delta = \dot{\epsilon} + \alpha \epsilon. \tag{23}$$

To guarantee obstacle clearance, we must introduce a robustifying term to the righthand side of (16) so that even in the presence of the greatest possible $\omega(t)$, the foot does not strike the obstacle.

Theorem 1. Consider the system with nominal error dynamics (14), a set of controls $\nu \in \mathbb{U} \subseteq \mathbb{R}^6$, and the closed set $\mathcal{C}_1 \subset \mathcal{D}_1 \subseteq \mathbb{X} \subseteq \mathbb{R}^{12}$ in (15), where \mathcal{D}_1 is given by (18) and the continuously differentiable function $h_1(\bar{x})$ is defined in (20). Let the error term $\omega(t) = [\epsilon^T, \delta^T, \chi^T, \varepsilon^T]^T \in \mathbb{R}^{14}$ be bounded as $||\omega_{\infty}|| \leq \bar{\omega}$. If ZCBF h_1 satisfies

$$L_f h_1(\bar{x}) + L_g h_1(\bar{x}) \nu \ge -\gamma_1 h_1(\bar{x})$$

$$+2 \left(||z_c - z_d + e||^2 + ||r - \alpha e||^2 \right),$$
(24)

for $\gamma_1 \in \mathbb{R}^+$, $\forall x \in \mathcal{D}_1$, then C_1' as defined in (19) is forward invariant.

Proof: The true h_1 is given by

$$h_1(x) = (z_1 - z_{c_1})^2 + (z_2 - z_{c_2})^2 - R^2 \ge 0.$$
 (25)

By (5) and (22), (25) can be reformulated as

$$h_1(x) = h_1(\bar{x}) - 2(z_d - e - z_c)^T \epsilon + ||\epsilon||^2 \ge 0.$$
 (26)

By (14), (20), and (23), the time derivative of (26) is

$$L_f h_1(x) + L_g h_1(x) \nu = L_f h_1(\bar{x}) + L_g h_1(\bar{x}) \nu + (27)$$

$$2(\epsilon^T (r - \alpha e) - (z_c - z_d + e)^T (\delta - \alpha \epsilon) + \epsilon^T (\delta - \alpha \epsilon)).$$

Using (24), (27) may be lower bounded as

$$L_{f}h_{1}(x) + L_{g}h_{1}(x)\nu \ge \gamma_{1}h_{1}(\bar{x}) - \frac{1}{2}||\delta||^{2}$$

$$-(\alpha + 2)||\delta|||\epsilon|| - (\frac{\alpha^{2}}{2} + 2\alpha + \frac{1}{2})||\epsilon||^{2}.$$
(28)

By Young's Inequality, $-||\delta||||\epsilon|| \ge -\frac{1}{2}(||\epsilon||^2 + ||\delta||^2)$. Hence,

$$L_{f}h_{1}(x) + L_{g}h_{1}(x)\nu \ge -\gamma_{1}h_{1}(\bar{x})$$

$$-\left(\frac{\alpha+3}{2}\right)||\delta||^{2} - \left(\frac{\alpha^{2}+5\alpha+3}{2}\right)||\epsilon||^{2}.$$
(29)

Defining $\zeta = \frac{\alpha^2 + 5\alpha + 3}{2}$, (29) may be bounded as

$$L_f h_1(x) + L_g h_1(x) \nu \ge -\gamma_1 h_1(\bar{x}) - \zeta ||\bar{\omega}||^2.$$
 (30)

Note that (30) is of the form of Eq. (26) in [27]. It follows that C_1' is forward invariant as long as $||\bar{\omega}||^2 < b^2 \gamma_1/\zeta$.

C. Fatigue Barrier Functions

Two barrier functions are imposed to limit ankle muscle fatigue. The fatigue constraints are given as

$$h_2(\bar{x}) = \bar{\mu}_{pf} - \mu_{0_{pf}}$$

$$h_3(\bar{x}) = \bar{\mu}_{df} - \mu_{0_{df}},$$
(31)

where $\mu_{0_j} \in [\mu_{minj}, \mu_{d_j}]$ is the minimum value of μ_j . (31) may be reformulated in terms of the states as

$$h_2(\bar{x}) = \tilde{\mu}_{pf} + \mu_{d_{pf}} - \mu_{0_{pf}}$$

$$h_3(\bar{x}) = \tilde{\mu}_{df} + \mu_{d_{df}} - \mu_{0_{df}}.$$
(32)

For Theorem 2, we define $\chi \in \mathbb{R}^6$, $\varepsilon \in \mathbb{R}^4$, respectively the activation and fatigue components of the disturbance, as

$$\varepsilon = \bar{\mu} - \mu, \quad \chi = \bar{a} - a.$$
 (33)

Theorem 2. Consider the system with nominal error dynamics (14), a set of controls $\nu \in \mathbb{U} \subseteq \mathbb{R}^6$, and the closed set $C_i \subset \mathcal{D}_i \subseteq \mathbb{X} \subseteq \mathbb{R}^{12}$ in (15), where \mathcal{D}_i is given by (18) and the continuously differentiable function $h_i(\bar{x})$ is defined in (31). Let the error term $\omega(t) = [\epsilon^T, \delta^T, \chi^T, \varepsilon^T]^T$ be bounded as $||\omega_{\infty}|| \leq \bar{\omega}$. If ZCBF h_i satisfies

$$L_{f}h_{i}(\bar{x}) + L_{g}h_{i}(\bar{x})\nu \ge -\gamma_{i}h_{i}(\bar{x}) + \frac{(\mu_{min_{i}} - \bar{\mu}_{i})^{2} + \bar{a}_{i}^{2}}{T_{f_{i}}} + \frac{(\bar{a}_{i} - 1)^{2} + (\bar{\mu}_{i} - 1)^{2}}{T_{r_{i}}},$$
(34)

for $\gamma_i \in \mathbb{R}^+$, $\forall x \in \mathcal{D}$, then C'_i as defined in (19) is forward invariant for i = 2, 3.

Proof: By (33), $h_i(x)$ is given by

$$h_{i}(x) = \mu_{i} - \mu_{0_{i}} = \bar{\mu}_{i} - \varepsilon_{i} - \mu_{0i}$$

$$= h_{i}(\bar{x}) - \varepsilon_{i} = h_{i}(\bar{x}) - \bar{\mu}_{i} + \mu_{i}.$$
(35)

Using (2), the time derivative of (35) is

$$L_{f}h_{i}(x) + L_{g}h_{i}(x)\nu = L_{f}h_{i}(\bar{x}) + L_{g}h_{i}(\bar{x})\nu$$

$$-\frac{1}{T_{f_{i}}}(\mu_{min_{i}}\chi_{i} - \bar{\mu}_{i}\bar{a}_{i} + \mu_{i}a_{i})$$

$$+\frac{1}{T_{c}}(\varepsilon_{i} + \chi_{i} - \bar{\mu}_{i}\bar{a}_{i} + \mu_{i}a_{i}).$$
(36)

By adding and subtracting $\mu_i \bar{a}_i$ and $\bar{\mu}_i \chi_i$, (36) becomes

$$L_{f}h_{i}(x) + L_{g}h_{i}(x)\nu = L_{f}h_{i}(\bar{x}) + L_{g}h_{i}(\bar{x})\nu$$

$$-\frac{\chi_{i}}{T_{f_{i}}}(\mu_{min_{i}} - \bar{\mu}_{i}) + \frac{\chi_{i}}{T_{r_{i}}}(1 - \bar{\mu}_{i}) + \frac{\varepsilon_{i}\bar{a}_{i}}{T_{f_{i}}}$$

$$+\frac{\varepsilon_{i}}{T_{r_{i}}}(1 - \bar{a}_{i}) + \left(\frac{1}{T_{r_{i}}} - \frac{1}{T_{f_{i}}}\right)\varepsilon_{i}\chi_{i}$$

$$(37)$$

By (34), completing the square, and Young's Inequality, (37) may be lower bounded as

$$L_{f}h_{i}(x) + L_{g}h_{i}(x)\nu \ge L_{f}h_{i}(\bar{x}) + L_{g}h_{i}(\bar{x})\nu$$

$$-\frac{1}{4}\left(\frac{1}{T_{f_{i}}} + \frac{1}{T_{r_{i}}} + 2\left|\frac{1}{T_{r_{i}}} - \frac{1}{T_{f_{i}}}\right|\right)||\bar{\omega}||^{2},$$
(38)

which is of the form of Eq. (26) in [27]. It follows that \mathcal{C}_i' is forward invariant for i=2,3 as long as $||\bar{\omega}||^2 < 4\gamma_i\mu_{0_i}/(\frac{1}{T_{f_i}}+\frac{1}{T_{r_i}}+2|\frac{1}{T_{r_i}}-\frac{1}{T_{f_i}}|)$.

IV. MPC FORMULATION

The MPC scheme is formulated as

$$\min_{\nu(t|t_k)} J^*(\bar{x}(t|t_k), \nu(t|t_k)) = \int_{t_k}^{t_k+T} l \, dt + V(\bar{x}(t_k + T|t_k))$$

$$\dot{\bar{x}}(t|t_k) = f(\bar{x}(t|t_k), \nu(t|t_k))$$

$$\bar{x}(t|t_k) \in \mathbb{X}$$

$$\bar{x}(t_{k+T}|t_k) \in \Omega_T$$

$$\nu(t|t_k) \in \mathbb{U}$$

$$u(t|t_k)_j \in [u_{min_j}, 1], \forall j$$

$$\dot{h}_1(\bar{x}(t|t_k), \nu(t|t_k)) \ge -\gamma_1 h_1(\bar{x}(t|t_k)) + \xi_1(\bar{x}(t|t_k)), i = 2, 3$$

$$\dot{h}_i(\bar{x}(t|t_k), \nu(t|t_k)) \ge -\gamma_i h_i(\bar{x}(t|t_k)) + \xi_i(\bar{x}(t|t_k)), i = 2, 3$$

$$(40)$$

for $t \in [t_k, t_{k+T}]$, constant prediction horizon T, $k = \mathbb{I}^+ \cup \{0\}$, $\mathbb{X} \subseteq \mathbb{R}^{12}$, $\mathbb{U} \subseteq \mathbb{R}^6$, and terminal region $\Omega_T \subseteq \mathbb{R}^{12}$. Note that $\dot{h}_i(\bar{x}(t|t_k), \nu(t|t_k))$ is used in place of $L_f h_i(\bar{x}(t|t_k)) + L_g h_i(\bar{x}(t|t_k)) \nu$ for simplicity, where, for a given variable v, $v(t|t_k)$ refers the value of v at future time t as predicted at time t_k . Recall that $u_{min_j} = 0, -1$ for FES and motors, respectively. The running cost t and terminal cost t are given by

$$l = \bar{x}^T Q \bar{x} + \nu^T R \nu$$

$$V = \frac{1}{2} e^T e + \frac{1}{2} r^T \bar{M}_z r + \frac{1}{2} e_x^T e_x + \frac{1}{2} \tilde{\mu}^T \tilde{\mu}$$

for positive definite, symmetric weight matrices $Q \in \mathbb{R}^{12 \times 12}$, $R \in \mathbb{R}^{6 \times 6}$. The terms $\xi_i \in \mathbb{R}$ are defined as

$$\xi_1(\bar{x}) = 2\Big(||z_c - z_d + e||^2 + ||r - \alpha e||^2\Big),$$

$$\xi_i(\bar{x}) = \frac{(\mu_{min_i} - \bar{\mu}_i)^2 + \bar{a}_i^2}{T_{f_i}}$$

$$+ \frac{(\bar{a}_i - 1)^2 + (\bar{\mu}_i - 1)^2}{T_{r_i}}, i = 2, 3.$$

V. RESULTS

Simulations were performed using a hybrid neuroprosthesis 3-link leg model with realistic musculoskeletal parameters from [28], [29]. After each optimization step, a 2 Hz sinusoidal disturbance of $48.3^{\circ}/s^2$ amplitude (15% of the maximum expected angular acceleration magnitude) was added to \ddot{q} , and its time integral was added to \dot{q} . Additionally, a 2 Hz sinusoidal disturbance of 0.025 amplitude was added to \dot{a} , and its time integral was added to $\dot{\mu}$. The stopping criterion for the MPC was $||\bar{z}-z_d||^2 \leq 0.0001$. Parameters were set as $\gamma_i=1500, \forall i,$

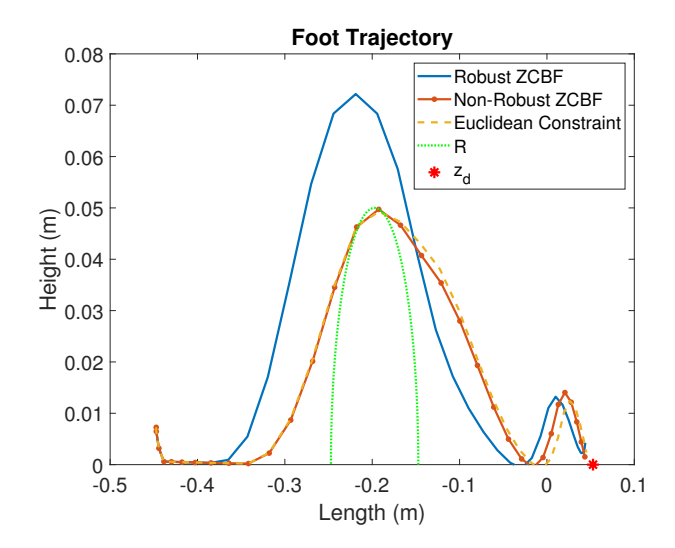


Fig. 1. Comparison of the foot trajectory for ZCBF with robustifying term, ZCBF without robustifying term, and with a simple Euclidean distance constraint.

 $\mu_{0_2} = \mu_{0_3} = 0.698$, and $\bar{\mu}_{pf}(t_0) = \bar{\mu}_{df}(t_0) = 0.7$. For our case, because the simulation occurred over a single swing phase, the minimum fatigue values μ_{0_i} were set very close to $\mu_i(t_0)$. In real-time application over the course of several steps, such a high value for μ_{0_i} would not be required for the fatigue ZCBF to affect control performance and safety.

Performance was compared with MPC using the ZCBFs without the robustifying term and with MPC using the constraints $h_i(\bar{x}) \geq 0$, i=1,2,3, in place of (39), (40). As evidenced by Fig. 1, the MPC with ZCBF was able to successfully clear the obstacle despite disturbances, while both the MPC with non-robust ZCBFs and MPC with a simple Euclidean safety constraint failed.

The effect of the ankle fatigue trajectories with robust ZCBFs can be seen in Fig. 2. When the robust fatigue ZCBFs are employed, both fatigue states remain above μ_0 . When only the robust obstacle clearance ZCBF is applied and fatigue is unconstrained, both fatigue states fall below μ_0 . For a longer time duration, such as the time required to complete several steps, the fatigue ZCBFs would play a more dramatic role in control input selection, yet their effectiveness is still evident in this small-time scale example.

VI. CONCLUSION AND FUTURE WORK

We have designed an MPC for a three-link hybrid neuroprosthesis that contains activation and fatigue dynamics. We constructed an obstacle clearance ZCBF so that the control does not require replanning of the time-varying desired trajectory. We also designed robustifying terms to withstand disturbances and modeling uncertainties, which are inevitable for user-specific hybrid neuroprostheses. Additionally, because ankle motors are not present in commercial powered exoskeletons, we formulated fatigue ZCBFs to constrain fatigue and avoid overstimulating the ankle muscles.

While the MPC with robust ZCBFs was able to successfully and quickly complete a step while remaining within the desired trajectory, future work will focus on proving recursive

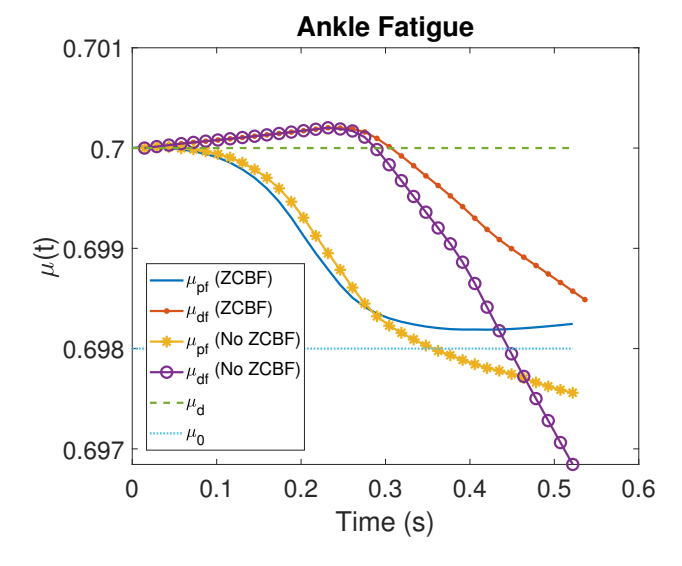


Fig. 2. Ankle plantar flexor (μ_{pf}) and dorsiflexor (μ_{df}) fatigue trajectories with and without robust fatigue ZCBFs. Both versions employ the robust obstacle clearance ZCBF.

feasibility and stability. Ellipsoidal barriers may prove useful for completing steps of desired height and length without replanning, and the MPC-ZCBF with obstacle avoidance holds promise for addressing tasks such as stair climbing.

REFERENCES

- A. Ekelem and M. Goldfarb, "Supplemental stimulation improves swing phase kinematics during exoskeleton assisted gait of sci subjects with severe muscle spasticity," *Frontiers in neuroscience*, vol. 12, p. 374, 2018.
- [2] N. Kapadia, K. Masani, B. Catharine Craven, L. M. Giangregorio, S. L. Hitzig, K. Richards, and M. R. Popovic, "A randomized trial of functional electrical stimulation for walking in incomplete spinal cord injury: effects on walking competency," *The journal of spinal cord medicine*, vol. 37, no. 5, pp. 511–524, 2014.
- [3] T. M. Kesar, R. Perumal, D. S. Reisman, A. Jancosko, K. S. Rudolph, J. S. Higginson, and S. A. Binder-Macleod, "Functional electrical stimulation of ankle plantarflexor and dorsiflexor muscles: effects on poststroke gait," *Stroke*, vol. 40, no. 12, pp. 3821–3827, 2009.
- [4] B. M. Doucet, A. Lam, and L. Griffin, "Neuromuscular electrical stimulation for skeletal muscle function," *The Yale journal of biology* and medicine, vol. 85, no. 2, p. 201, 2012.
- [5] N. A. Kirsch, X. Bao, N. A. Alibeji, B. E. Dicianno, and N. Sharma, "Model-based dynamic control allocation in a hybrid neuroprosthesis," *IEEE Transactions on Neural Systems and Rehabilitation Engineering*, vol. 26, no. 1, pp. 224–232, 2017.
- [6] A. J. Del-Ama, Á. Gil-Agudo, J. L. Pons, and J. C. Moreno, "Hybrid FES-robot cooperative control of ambulatory gait rehabilitation exoskeleton," *Journal of neuroengineering and rehabilitation*, vol. 11, no. 1, pp. 1–15, 2014.
- [7] K. H. Ha, S. A. Murray, and M. Goldfarb, "An approach for the cooperative control of FES with a powered exoskeleton during level walking for persons with paraplegia," *IEEE Transactions on Neural Systems and Rehabilitation Engineering*, vol. 24, no. 4, pp. 455–466, 2015
- [8] X. Bao, Z. Sheng, B. E. Dicianno, and N. Sharma, "A tube-based model predictive control method to regulate a knee joint with functional electrical stimulation and electric motor assist," *IEEE Transactions on Control Systems Technology*, vol. 29, no. 5, pp. 2180–2191, 2020.
- [9] V. Molazadeh, Q. Zhang, X. Bao, B. E. Dicianno, and N. Sharma, "Shared control of a powered exoskeleton and functional electrical stimulation using iterative learning," Frontiers in Robotics and AI, vol. 8, 2021.
- [10] Z. Sun, X. Bao, and N. Sharma, "Tube-based model predictive control of an input delayed functional electrical stimulation," in 2019 American Control Conference (ACC). IEEE, 2019, pp. 5420–5425.

- [11] D. H. Gagnon, M. J. Escalona, M. Vermette, L. P. Carvalho, A. D. Karelis, C. Duclos, and M. Aubertin-Leheudre, "Locomotor training using an overground robotic exoskeleton in long-term manual wheelchair users with a chronic spinal cord injury living in the community: Lessons learned from a feasibility study in terms of recruitment, attendance, learnability, performance and safety," *Journal of neuroengineering and rehabilitation*, vol. 15, no. 1, pp. 1–12, 2018.
- [12] S. Wang, B. Zhang, Z. Yu, and Y. Yan, "Differential soft sensor-based measurement of interactive force and assistive torque for a robotic hip exoskeleton," *Sensors*, vol. 21, no. 19, p. 6545, 2021.
- [13] G. Serrancolí, A. Falisse, C. Dembia, J. Vantilt, K. Tanghe, D. Lefeber, I. Jonkers, J. De Schutter, and F. De Groote, "Subject-exoskeleton contact model calibration leads to accurate interaction force predictions," *IEEE Transactions on Neural Systems and Rehabilitation Engineering*, vol. 27, no. 8, pp. 1597–1605, 2019.
- [14] D.-X. Liu, J. Xu, C. Chen, X. Long, D. Tao, and X. Wu, "Vision-assisted autonomous lower-limb exoskeleton robot," *IEEE transactions on systems, man, and cybernetics: systems*, vol. 51, no. 6, pp. 3759–3770, 2019.
- [15] M. Khalili, H. M. Van der Loos, and J. F. Borisoff, "Studies on practical applications of safe-fall control strategies for lower limb exoskeletons," in 2019 IEEE 16th International Conference on Rehabilitation Robotics (ICORR). IEEE, 2019, pp. 536–541.
- [16] B. C. Allen, K. J. Stubbs, and W. E. Dixon, "Saturated control of a switched fes-cycle with an unknown time-varying input delay," *IFAC-PapersOnLine*, vol. 53, no. 5, pp. 403–408, 2020.
- [17] C. A. Rouse, C. A. Cousin, B. C. Allen, and W. E. Dixon, "Shared control for switched motorized FES-cycling on a split-crank cycle accounting for muscle control input saturation," *Automatica*, vol. 123, p. 109294, 2021.
- [18] A. Isaly, B. C. Allen, R. G. Sanfelice, and W. E. Dixon, "Encouraging volitional pedaling in functional electrical stimulation-assisted cycling using barrier functions," *Frontiers in Robotics and AI*, vol. 8, 2021.
- [19] A. D. Ames, X. Xu, J. W. Grizzle, and P. Tabuada, "Control barrier function based quadratic programs for safety critical systems," *IEEE Transactions on Automatic Control*, vol. 62, no. 8, pp. 3861–3876, 2016.
- [20] J. Zeng, Z. Li, and K. Sreenath, "Enhancing feasibility and safety of nonlinear model predictive control with discrete-time control barrier functions," in 2021 60th IEEE Conference on Decision and Control (CDC). IEEE, 2021, pp. 6137–6144.
- [21] R. Grandia, A. J. Taylor, A. Singletary, M. Hutter, and A. D. Ames, "Nonlinear model predictive control of robotic systems with control lyapunov functions," arXiv preprint arXiv:2006.01229, 2020.
- [22] J. Zeng, B. Zhang, and K. Sreenath, "Safety-critical model predictive control with discrete-time control barrier function," in 2021 American Control Conference (ACC). IEEE, 2021, pp. 3882–3889.
- [23] T. D. Son and Q. Nguyen, "Safety-critical control for non-affine non-linear systems with application on autonomous vehicle," in 2019 IEEE 58th Conference on Decision and Control (CDC). IEEE, 2019, pp. 7623–7628.
- [24] Q. Nguyen, A. Hereid, J. W. Grizzle, A. D. Ames, and K. Sreenath, "3d dynamic walking on stepping stones with control barrier functions," in 2016 IEEE 55th Conference on Decision and Control (CDC). IEEE, 2016, pp. 827–834.
- [25] G. York and S. Chakrabarty, "A survey on foot drop and functional electrical stimulation," *International Journal of Intelligent Robotics and Applications*, vol. 3, no. 1, pp. 4–10, 2019.
- [26] F. Sharif, S. Ghulam, A. N. Malik, and Q. Saeed, "Effectiveness of functional electrical stimulation (FES) versus conventional electrical stimulation in gait rehabilitation of patients with stroke," *J Coll Physi*cians Surg Pak, vol. 27, no. 11, pp. 703–706, 2017.
- [27] S. Kolathaya and A. D. Ames, "Input-to-state safety with control barrier functions," *IEEE control systems letters*, vol. 3, no. 1, pp. 108–113, 2018.
- [28] D. Popovic, R. B. Stein, M. N. Oguztoreli, M. Lebiedowska, and S. Jonic, "Optimal control of walking with functional electrical stimulation: a computer simulation study," *IEEE Transactions on Rehabilitation Engineering*, vol. 7, no. 1, pp. 69–79, 1999.
- [29] S. Dosen and D. B. Popovic, "Moving-window dynamic optimization: design of stimulation profiles for walking," *IEEE Transactions on Biomedical Engineering*, vol. 56, no. 5, pp. 1298–1309, 2009.